Triple Halide Bridges in Chiral $Mn^{II}_2Mn^{III}_6Na^{I}_2$ Cages: Structural and Magnetic Characterization

Júlia Mayans,[†] Mercè Font-Bardia,[‡,§] and Albert Escuer[*,†]

† Departament de Química Inorgànica i Orgànica, Secció Inorgànica and Institut de Nanociència i Nanotecnologia, Universitat de Barcelona, Martí i Franqués 1−11, Barcelona 08028, Spain
‡ Departament de Mineralogia, Cristal·lografia i Dipòsits Minerals, Universitat de Barcelona, Martí Franqués s/n, 08028 Barcelona, Spain
§ Unitat de Difraccióde R-X, Centre Científic i Tecnològic de la Universitat de Barcelona, Soléi Sabarís 1−3, 08028 Barcelona, Spain

ABSTRACT:

A family of decanuclear chiral clusters with a MnII 2MnIII 6NaI 2 core have been synthesized from enantiomerically pure Schiff bases. The new systems consist of two MnIIMnIII 3NaI units linked by rare triple chloro or bromo bridges between the divalent Mn cations. Susceptibility measurements point out the weak antiferromagnetic interaction mediated by these kinds of bridges and afford the first magnetic measurements for the (μ-Br)3 case.

Multidentate Schiff bases obtained from the condensation of o-vanillin and amino alcohols have been widely employed in coordination chemistry (around 180 entries in CCDC) because of their good chelating properties with 3d or 4f cations. The large variety of easily available amino alcohols has been useful in modulating the size, charge, or number of O-atom donors resulting in H2L, H3L, or H4L Schiff bases as a function of the adequate choice of the starting reagent 2-amino-1- ethanol,1−5 3-amino-1,2-propanediol,6−10 2-amino-2-methyl- 1,3-propanediol,3 or tris(hydroxymethyl)aminomethane.11

One characteristic kind of complex derived of these ligands in manganese chemistry consists of [MnIII 3MnIINaI] cages, in which the cations determine a trigonal bipyramid defined by one {(μ3- O)MnIII 3} triangle with NaI and MnII cations in the apical positions. Among them, two kinds of complexes can be differentiated as a function of the employed Schiff base: the H3L ligands derived from condensation with 3-amino-1,2- propanediol,6−10 which generate two octahedral cavities that satisfy all of the coordination sites of the apical MnII and NaI cations (Chart 1; H3L-A type) and the H2L ligands derived from 2-amino-1-ethanol, or in some random cases H3L or H4L, which maintain the cavity for the NaI ion but not for the MnII cation, which, after formation of the cage, still has an open face capable of coordinating additional ligands (Chart 1, H2L-B type). Usually, these coordination sites are occupied by anions or solvent molecules, but two pentanuclear units are able to share their open faces by means of triple bridges, as has been reported in two cases for the μ1,1-N3 ligand.4,10

An additional interest of H2L-B kinds of ligands is that chirality can be incorporated by substitution on the C atoms of the hydroxyethyl fragment and enantiomerically pure chiral bases can be easily obtained from the substituted (R)- or (S)-2-amino- 1-ethanol.

Following our work in this field,5,12 we have explored the reactivity in manganese chemistry of the enantiomerically pure (R)- and (S)-H2L ligands derived from the condensation of ovanillin and 2-amino-3-methyl-1-butanol (Chart 2), which remains unexplored in 3d coordination chemistry (only one meso-[Ni4L4] cubane13 has been reported to date). The reason for this choice was to check its reactivity in comparison with other members of this family of ligands because the substituent is not innocent and different clusters or nuclearities can be obtained.

The reaction of H2L with manganese halides in a methanolic solution allowed characterization of the first manganese derivatives of H2L consisting of two enantiomeric decanuclear anionic clusters with the formula Na[Mn8Na2(L)6(O)2(Cl)9] (1R and 1S) and the pair of enantiomers of the related complex with bromo ligands Na[Mn8Na2(L)6(O)2(Br)9] (2R and 2S). See the Supporting Information for synthetic details. The core of these complexes consists of two [MnIII 3MnIINaI] cages linked by the extremely unusual triple halide MnII−(X)3−MnII bridge. The new compounds have been characterized by X-ray diffraction, electronic circular dichroism (ECD), and magnetic susceptibility measurements. The structures are very similar; therefore, only a common description based on 1R is provided. Crystal data for 1R and 1S are summarized in Table S1. Selected bond parameters for 1R and 1S are listed in Tables S2 and S3. The cell and some significant bond parameters for the isostructural complex 3S are

also provided in Tables S1 and S5. The oxidation states of the Mn atoms have been assigned by structural considerations and bondvalence- sum calculations (Table S4).

Compound 1R consists of two trigonal-bipiramidal [MnIII 3MnIINaI] clusters joined by a triple μ-Cl bridge that links the MnII cations. A view of the cluster and a labeled core can be seen in Figure 1. Each pentanuclear subunit consists of a μ3-Ocentered equilateral triangle of MnIII cations, one MnII cation, and one NaI cation in the apical positions of the trigonal bipyramid. These cations are held together by three L2− ligands that link the NaI cation with the MnIII ions by means of the phenoxide O atom and the MnIII with the MnII cations with the alkoxide O-atom donors (Chart 2). The coordination polyhedron around the MnIII cations is an elongated octahedron with two trans-μ-Cl ligands in the axial coordination sites. Coordination is completed with one μ3-O donor placed in the center of the triangle. The three methoxide and phenoxide Oatom donors form a cavity that holds the NaI cations.

The two [MnIII 3MnIINaI] subunits are not equivalent and show different bond parameters (Table S2). The oxo donor O7 is placed in the center of the triangle determined by Mn1 (and symmetry-related cations) and acts as a μ3-O, whereas O8 is displaced by 0.262 Å out of the mean MnIII 3 plane determined by Mn2 (and symmetry-related cations) toward the NaI cation, resulting in a Na2−O8 distance of 2.605 Å and, thus, O8 can be assumed as a μ4-O bridge. SHAPE14 measurements show that the coordination polyhedron around Na1 is very close to a trigonal prism, but it is closer to an octahedron for Na2 (Figure 2 and Table S6). An axial view of the clusters shows that, taking the [OMnIII 3Cl3] mean plane as a reference, the two subunits are slightly deviated from an eclipsed configuration (determined by the sharing of one face of the MnII coordination polyhedra), in contrast with the related systems that consist of two [MnIIIMNaI] units sharing the M cation (M = MnII, LnIII),5,15 which always show a staggered conformation.

Transfer of the chirality from the chiral centers to the coordination sphere of the cations or the whole molecule is a common effect that, in this case, can be seen at the level of opposite helicity of the propeller-shaped [MnIII 3MnIINaI] units or the opposite Δ/Λ conformation of the chiral NaI cations (Figure 2).

These structural results point out that the resulting complexes are sensitive to the substituents on the hydroxyethyl C atoms. Equivalent reactions with the ligand with one phenyl group instead of isopropane produce one nonanuclear system formed by the same subunits but sharing the MnII cation.5 Interestingly, the reported systems with triple bridges (azido) have also been obtained from ligands with methyl or alkoxo substituents.4,10

The ECD spectra for the two pairs of enantiomers 1R/1S and 2R/2S measured in a methanolic solution show similar plots and are perfect mirror images among them, as must be expected from isostructural enantiomerically pure compounds (Figure 3). The spectrum of (R)-H2L shows two positive absorptions centered at 213 and 275 nm, three negative bands at 227, 248(w), and 314(w) nm associated with the π−π* transitions, and no bands in the visible region. The spectra of the reported complexes exhibit bands with the same sign in the UV region due to the coordinated L−2 ligand, strong new absorptions around

380 and 425 nm, and weak broad absorptions up to 700 nm that suggest the participation of molecular orbitals, with contribution of the MnIII cations that are directly linked to the aromatic groups. A comparison between the spectra of the chloro or bromo complexes shows identical spectra, and thus any effect related with these ligands or the MnII cation, linked to the aliphatic moiety of the ligand, must be expected.

Susceptibility measurements were performed on powdered samples of one chloro and one bromo complexes. The room temperature χMT values for 1R and 2S are 21.8 and 24.0 cm3· mol−1·K, respectively, lower than the calculated value of 26.75 cm3·mol−1·K for two MnII and six MnIII isolated cations (g = 2.00; Figure 4). Upon cooling, χMT decreases continuously to values of 3.60 or 9.91 cm3·mol−1·K at 2 K for 1R or 2S, respectively.

The complexes possess C3 symmetry, and assuming that both subunits contribute equally to the magnetic response, a simplified coupling scheme with only three different superexchange pathways (MnIII···MnIII, J1; MnII···MnIII, J2; MnII···MnII, J3) can be proposed to fit the experimental data (see Figure S3 for the coupling scheme and the applied isotropic Hamiltonian).

Fitting of the experimental data was performed with the PHI16 program in the 300−2 K range of temperatures, and best-fit parameters were J1 = +2.0 cm−1, J2 = −7.8 cm−1, J3 = −2.6 cm−1, and g = 1.91 with R = 8.5 × 10−4 for 1R and J1 = +7.2 cm−1, J2 = −6.4 cm−1, J3 = −0.3 cm−1, and g = 1.89 with R = 1.9 × 10−4 for 2S. These values indicate ferromagnetic interaction inside the MnIII 3 triangles and antiferromagnetic (AF) interaction with the MnII cations, resulting in a local S = 7/2 for each subunit. The weak AF interaction mediated by the triple halide bridge led to a final S = 0 ground state with very close S ≠ 0 levels for 1R, whereas the response of 2S is closer to the sum of two quasiisolated MnIIMnIII 3 fragments. In agreement with these data, the magnetization plot for 1R shows a continuous increase of the magnetization with a change of slope around 1 T, reaching the unsaturated value of 7.1 Nμβ under the maximum field of 5 T, whereas the magnetization plot for 2S tends to a quasi-saturated value of 11.8 Nμβ, slightly lower than the sum of two isolated {(μ3-O)MnIIMnIIINaI} fragments (12.6 Nμβ for the g = 1.90 value found in the susceptibility measurement).

Magnetic measurements for triple chloro bridges between MnII cations have only been reported for three [MnCl3]− chains17−19 with Mn−Cl−Mn bond angles comprised between 77.5 and 78.4° and similar J values (−4.8/−5.5 cm−1) and for one discrete molecular dimer reported by Wieghardt et al.20 for which a J value of −11.6 cm−1 was found for an average Mn−Cl−Mn bond angle of 74.4°. Our value of −2.6 cm−1 for the bond angle of 76.2° is comparable with these data. In contrast, any measure has never been reported for structurally characterized triple bromo bridges and thus any comparison can be made. The only data for a Mn−(Br)3−Mn fragment were reported in a partially characterized dimer for which a weak AF interaction was proposed.20 In light of our results, there is evidence for a weak AF interaction promoted by triple chloro or bromo bridges, being clearly lower for the bromo case.

The MnIII coordination polyhedron is elongated toward the chloro donors and, thus, the easy axis lies in the {μ3O−Mn3 III} plane, forming angles of around 60° between them. This arrangement cancels the

anisotropy, and as was experimentally checked, no out-of-phase response was found in alternatingcurrent experiments.

In conclusion, the reported systems reveal or confirm several unusual features: (a) evidence of the versatility of these kinds of ligands as a function of the substituents on the aliphatic C atoms; (b) the first examples of manganese complexes with H2L and their first chiral derivatives; (c) the second molecular compound with a triple chloro bridge between Mn atoms and the first one with triple bromo bridges; (d) magnetic susceptibility measurements confirming the ferromagnetic response for the unusual {MnIII 3(μ-Cl)3(μ3-O)} triangles and evidence of the weak AF interaction promoted by the triple bridge, with the interaction being stronger for (μ-Cl)3 than for (μ-Br)3.

AUTHOR INFORMATION

Corresponding Author

*E-mail: albert.escuer@ub.edu.

ORCID

Albert Escuer: 0000-0002-6274-6866

Notes

The authors declare no competing financial interest.

ACKNOWLEDGEMENTS

Funds from the Ministerio de Economia y Competitividad under Project CTQ2015-63614-P are acknowledged.

REFERENCES

(1) Gole, B.; Mondal, K. C.; Mukherjee, P. S. Tuning nuclearity of clusters by positional change of functional group: Synthesis of polynuclear clusters, crystal structures and magnetic properties. Inorg. Chim. Acta 2014, 415, 151−164.

(2) Fan, L.-L.; Guo, F.-S.; Yun, L.; Lin, Z.-J.; Herchel, R.; Leng, J.-D.; Ou, Y.-C.; Tong, M.-L. Chiral transition metal clusters from two enantiomeric schiff base ligands. Synthesis, structures, CD spectra and magnetic properties. Dalton Trans. 2010, 39, 1771−1780.

(3) Hewitt, I. J.; Tang, J.-K.; Madhu, N. T.; Clerac, R.; Buth, G.; Anson, C. E.; Powell, A. K. A series of new structural models for the OEC in photosystem II. Chem. Commun. 2006, 2650−2652.

(4) Song, Y.; Zhang, G.; Qin, X.; Gao, Y.; Ding, S.; Wang, Y.; Du, C.; Liu, Z. Chiral [NaMnIIMnIII 3] and [Na2MnII 2MnIII 6] clusters constructed by chiral multidentate Schiff-base ligands: synthesis, structures, CD spectra and magnetic properties. Dalton Trans. 2014, 43, 3880−3887.

(5) Escuer, A.; Mayans, J.; Font-Bardia, M.; Górecki, M.; Di Bari, L. Syntheses, structures, chiroptical and magnetic properties of chiral clusters built from Schiff bases: a novel [MnIIMnIII 6NaI 2] core. Dalton Trans. 2017, 46, 6514−6517.

(6) Nayak, S.; Nayek, H. P.; Dehnen, S.; Powell, A. K.; Reedijk, J. Trigonal propeller-shaped [MnIII 3MIINa] complexes (M = Mn, Ca): structural and functional models for the dioxygen evolving centre of PSII. Dalton Trans. 2011, 40, 2699−2702.

(7) Ding, C.; Gao, C.; Ng, S.; Wang, B.; Xie, Y. Polynuclear complexes with alkoxo and phenoxo bridges from in situ generated hydroxy-rich Schiff base ligands: syntheses, structures, and magnetic properties. Chem. - Eur. J. 2013, 19, 9961−9972.

(8) Cong, L.; Qin, X.; Sun, W.; Wang, Y.; Ding, S.; Liu, Z. A series of [NaMnIII 3MnII] clusters constructed using a multidentate Schiff-base ligand and decorated with different auxiliary ligands. New J. Chem. 2014, 38, 545−551.

(9) Yang, P.-P.; Zhu, L.-L.; Xu, Y.; Shao, C.-Y. Synthesis, crystal structures, and magnetic properties of two tetrahedral MnIIMnIII 3 complexes. Z. Anorg. Allg. Chem. 2013, 639, 1821−1826.

(10) Yang, P.-P.; Shao, C.-Y.; Zhu, L.-L.; Xu, Y. Syntheses, crystal structures, and magnetic properties of a family of tetra- and octanuclear mixed-valent manganese clusters. Eur. J. Inorg. Chem. 2013, 2013, 5288−5296.

(11) Liu, D.; Zhou, Q.; Chen, Y.; Yang, F.; Yu, Y.; Shi, Z.; Feng, S. Constructing octa- and hexadecanuclear manganese clusters from tetrahedral MnIII 3MnII cores bridged by quinquedentate Schiff base and versatile azide groups. Dalton Trans. 2010, 39, 5504−5508.

(12) Escuer, A.; Mayans, J.; Font-Bardia, M.; Di Bari, L.; Górecki, M. Mn3 III complexes derived from R/S-Schiff bases: chiral Single-Molecule-Magnets. Eur. J. Inorg. Chem. 2017, 2017, 991−998.

(13) Karmakar, S.; Khanra, S. Polynuclear coordination compounds: a magnetostructural study of ferromagnetically coupled Ni4O4 cubane core motif. CrystEngComm 2014, 16, 2371−2383.

(14) Llunell, M.; Casanova, D.; Cirera, J.; Alemany, P.; Alvarez, S. SHAPE, version 2.0; Barcelona, 2010. The program can be obtained by request to the authors.

(15) Yang, P.-P.; Wang, X.-L.; Li, L.-C.; Liao, D.-Z. Synthesis, structure and magnetic properties of a novel family of heterometallic nonanuclear NaI 2MnIII 6LnIII (Ln = Eu, Gd, Tb, Dy) complexes. Dalton Trans. 2011, 40, 4155−4161.

(16) Chilton, N. F.; Anderson, R. P.; Turner, L. D.; Soncini, A.; Murray, K. S. PHI: a powerful new program for the analysis of anisotropic monomeric and exchange-coupled polynuclear d- and fblock complexes. J. Comput. Chem. 2013, 34, 1164−1175.

(17) Caputo, R. E.; Roberts, S.; Willett, R. D.; Gerstein, B. C. Crystal structure and magnetic susceptibility of [(CH3)3NH]3Mn2Cl7. Inorg. Chem. 1976, 15, 820−823.

(18) Caputo, R. E.; Willett, R. D. Crystal structure and magnetic susceptibility of (CH3)2NH2MnCl3 (DMMC): A low-symmetry analog of (CH3)4NMnCl3 (TMMC). Phys. Rev. B 1976, 13, 3956−3961.

(19) Tancharakorn, S.; Fabbiani, F. P. A.; Allan, D. R.; Kamenev, K. V.; Robertson, N. Combined magnetic and single-crystal X-ray structural tudy of the linear chain antiferromagnet [(CH3)4N][MnCl3] under varying pressure. J. Am. Chem. Soc. 2006, 128, 9205−9210.

(20) Bossek, U.; Nuhlen, D.; Bill, E.; Glaser, T.; Krebs, C.; Weyhermuller, T.; Wieghardt, K.; Lengen, M.; Trautwein, A. X. Exchange coupling in an isostructural series of face-sharing

256 bioctahedral complexes [LMII(μ-X)3MIIL]BPh4 (M = Mn, Fe, Co, Ni, Zn; X = Cl, Br; L =
257 1,4,7-trimethyl-1,4,7-triazacyclononane). Inorg. Chem. 1997, 36, 2834−2843.

258

259

Legends to figures

Chart 1. Schematic Drawing of the Typical [MnIII3MnIINaI] Cages with a Closed Pocket around the MnII Cation (H3L-A) or Open-Face MnII Cation (H2L-B)a

Chart 2. Schematic Drawing of the Anionic Form of the H2L Ligand Employed in This Work and Its Coordination to the Metallic Centersa

Figure. 1. (Top) View of complex 1R. (Bottom) Labeled core of 1R.

Scheme 4 Oxidative addition of methyl iodide followed by isomerisation.

Scheme 5 Proposed species formed in solution (the charges of the ionic species are omitted).

Figure. 2. Mirror image of the helical arrangement of the ligands for 1R (left) and 1S (right) and a view of the coordination of the corresponding Na1 (top) and Na2 (bottom) cations.

Figure. 3. ECD spectra in a methanolic solution for complexes 1R, 1S, 2R, and 2S.

Figure. 4 χMT product vs. temperature for complexes 1R (squares) and 2S (circles). Inset, magnetization plot for 1R and 2S.

CHART 1

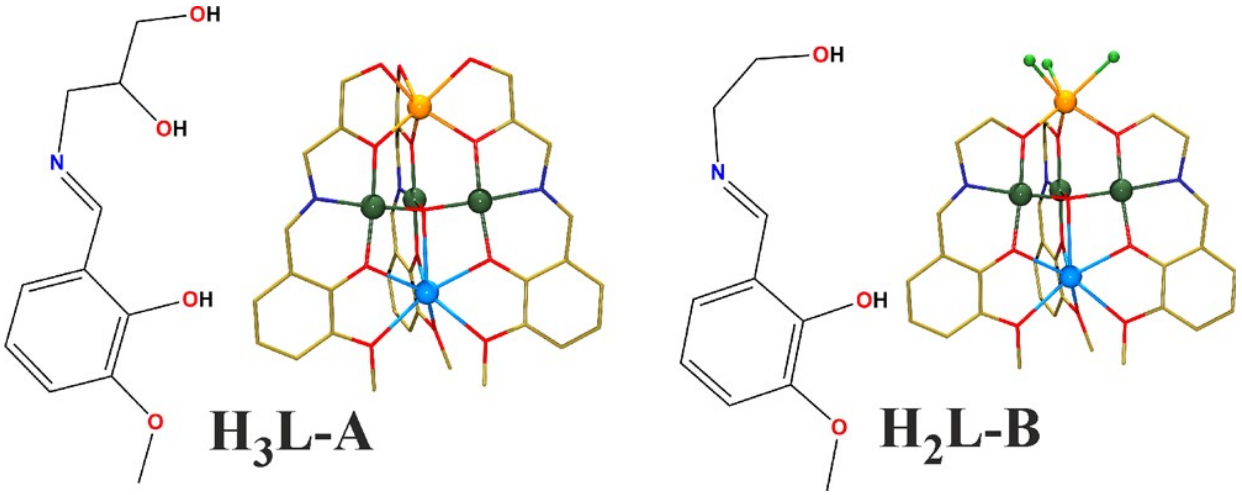

[a]Color code for all plots: O, red; N, navy blue; NaI, blue; MnII, orange; MnIII, dark green; Cl, violet.

290 **CHART 2**

291

292

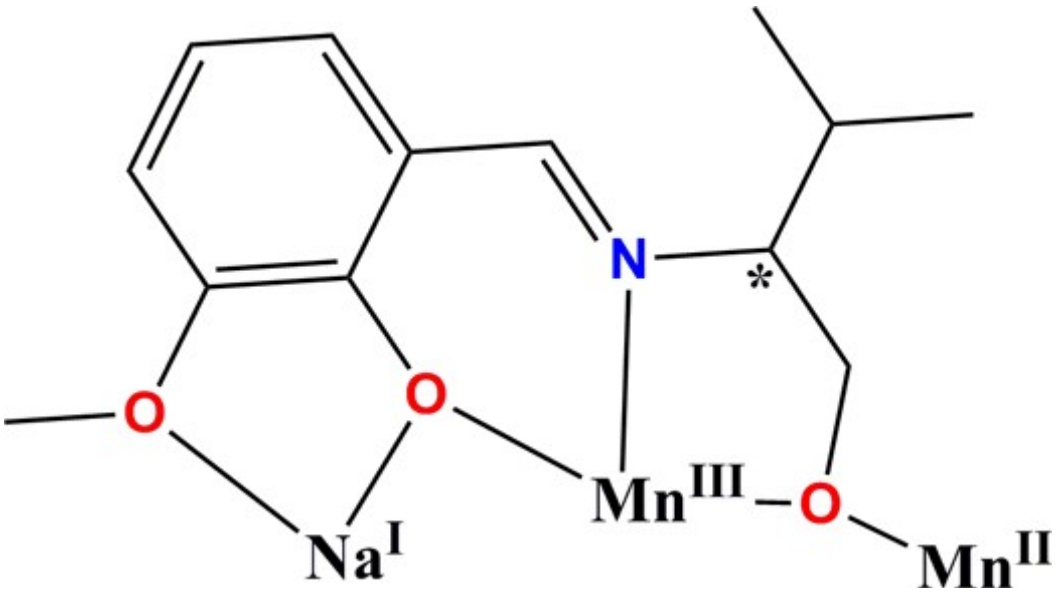

293

294

295

296 [a]The asterisk denotes the chiral C atom.

297

298 **FIGURE 1**

299

300

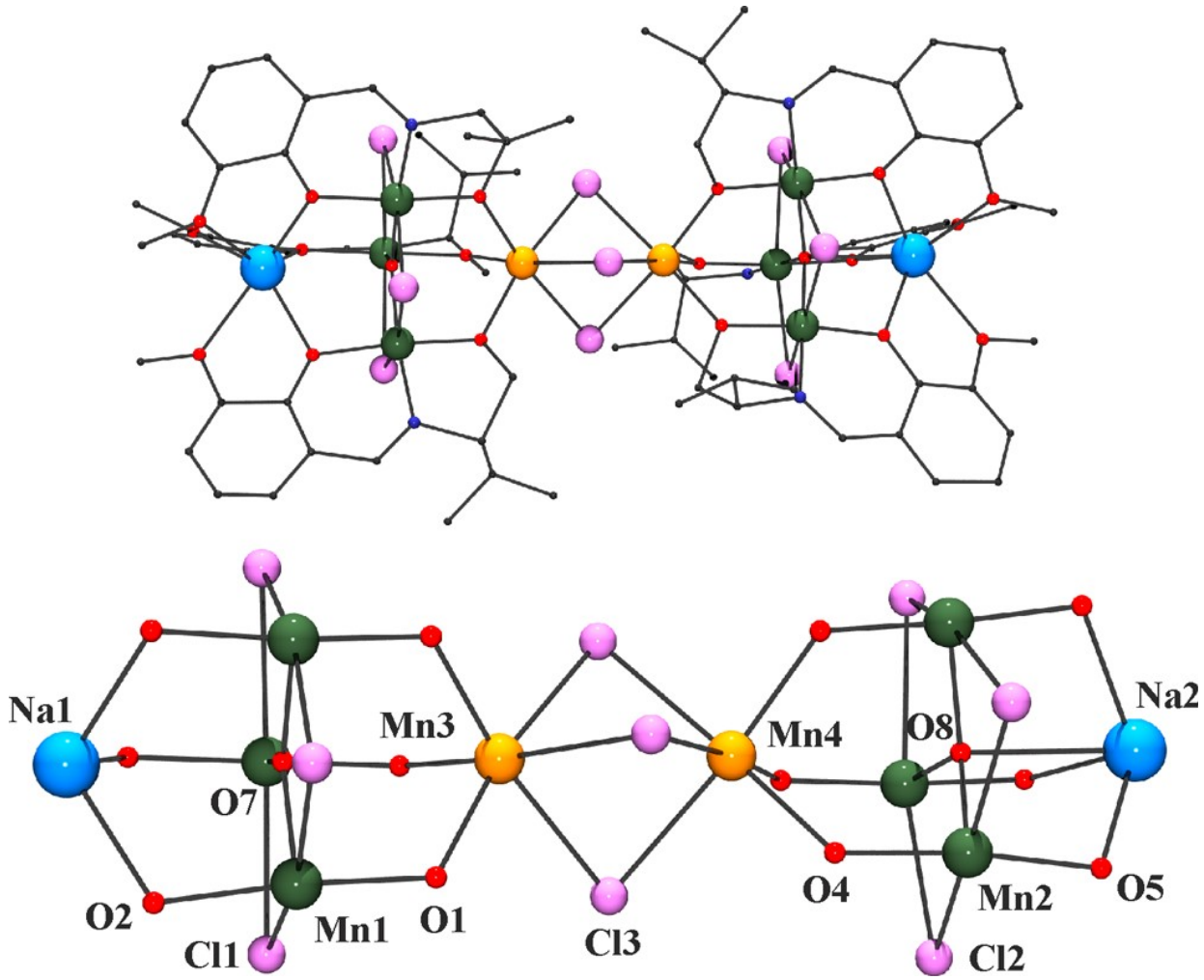

301

302

FIGURE 2

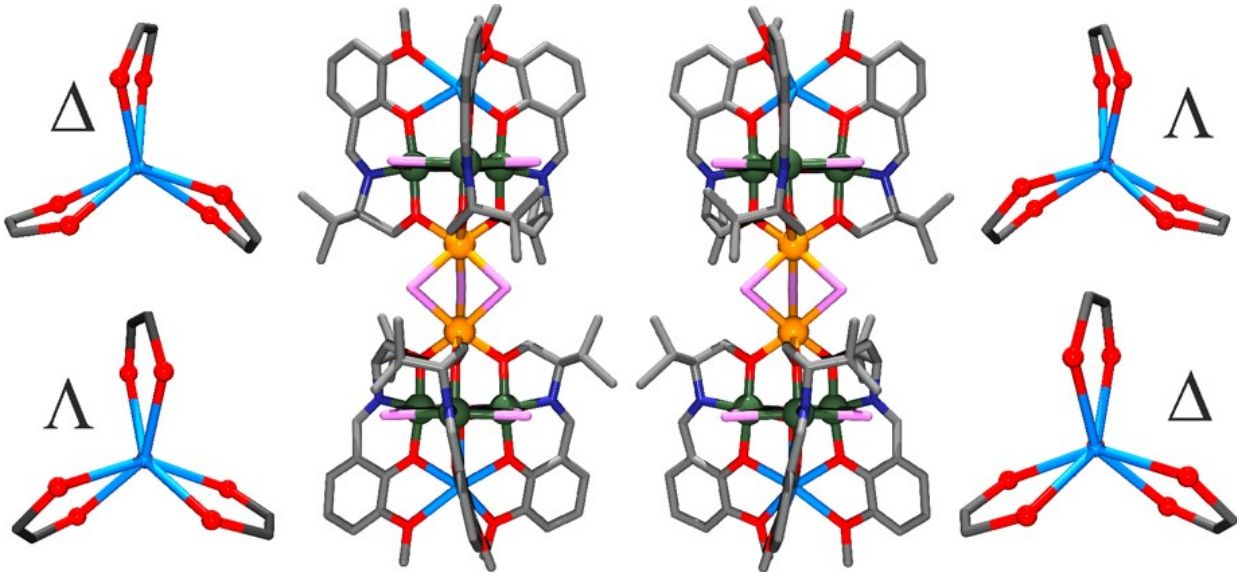

308 **FIGURE 3**

309

310

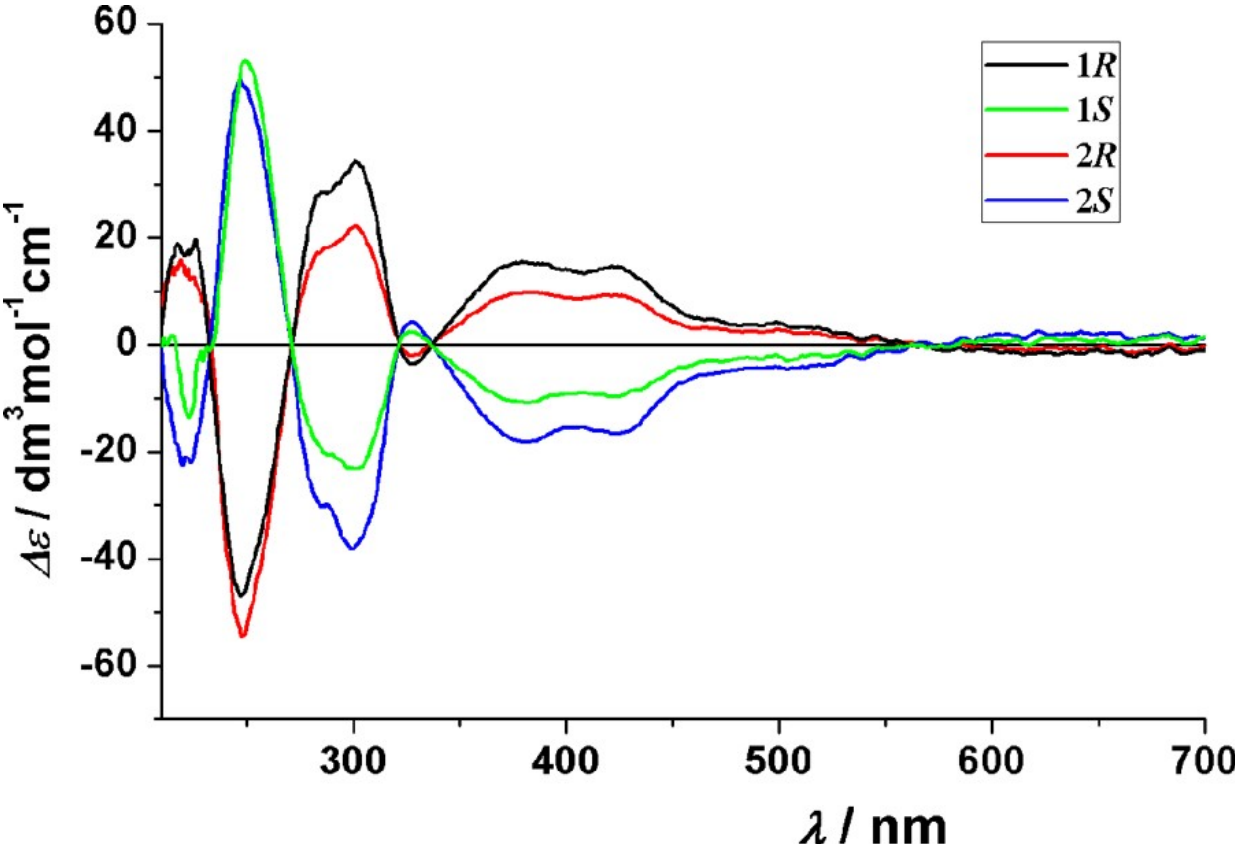

311

312

313 **FIGURE 4**

314

315

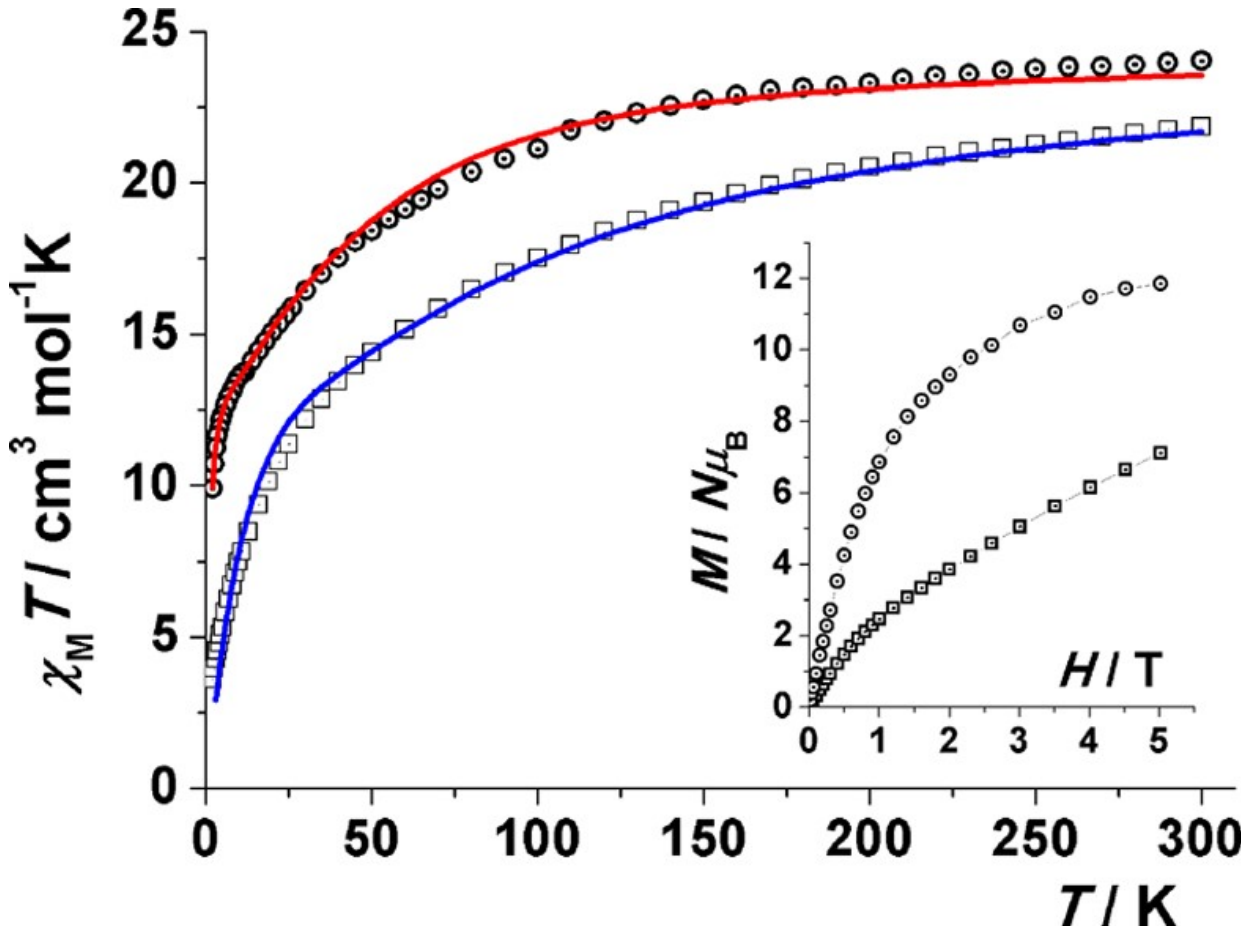

316